

# Ultrafine Spinel Powders by Flame Spray Pyrolysis of a Magnesium Aluminum Double Alkoxide

Clint R. Bickmore,\* Kurt E. Waldner, David R. Treadwell,\* and Richard M. Laine\*†

Department of Materials Science and Engineering, and Department of Chemistry, University of Michigan, Ann Arbor, Michigan 48109-2136

Ultrafine crystalline spinel powder has been prepared using flame spray pyrolysis of alcoholic solutions of a novel double alkoxide precursor. The particles produced are spherical, dense, single crystals with diameters of 10–100 nm and specific surface areas ranging from 40 to 60 m<sup>2</sup>/g. Powder production rates of 50–100 g/h are achieved using a bench-top apparatus. Particle formation appears to occur by rapid oxidation of the organic ligands followed by nucleation and growth from oxide species.

## I. Introduction

THE field of ultrafine ceramic powders, wherein the primary particle size is less than 100 nm, has grown rapidly in the last decade. The primary driving force for this growth is the possibility of obtaining exceptional properties from ceramics with an ultrafine grain structure including transparency,<sup>1</sup> superplasticity and creep properties,<sup>2</sup> and low-temperature sintering.<sup>3,4</sup> Numerous techniques are available for the production of both oxide and non-oxide<sup>5</sup> ultrafine ceramic powders. These may be divided into three categories: (1) solid–vapor–solid, (2) liquid–vapor–solid, (3) liquid–solid. Examples include the following: (Type 1) metal oxide vapor condensation,<sup>6</sup> metal vapor condensation and oxidation,<sup>7</sup> laser ablation,<sup>8</sup> sputtering,<sup>8</sup> plasma-assisted chemical vapor deposition;<sup>5b</sup> (Type 2) spray,<sup>9</sup> electrospray,<sup>10</sup> and flame spray pyrolysis of metal salt and metallo-organic solutions;<sup>4,11</sup> and (Type 3) precipitation from salt<sup>12</sup> and metallo-organic solutions.<sup>13</sup> One of the limiting factors in the wide-scale use of high-purity, ultrafine ceramic powders (other than a few single-component oxides, e.g., fumed silica, long in commercial production) is the high cost associated with producing these powders as a result of (1) relatively low production rates, (2) capital-intensive equipment, and (3) expensive starting materials.

We have recently developed direct synthetic routes to a wide variety of inexpensive ceramic precursors from the corresponding metal oxides or hydroxides.<sup>14</sup> In a very simple “one-pot” synthesis process, alkoxide precursors containing any combination of Al, Si, with or without Group I or II metals, are readily produced. In this work, a precursor to spinel<sup>15</sup> (MgAl<sub>2</sub>O<sub>4</sub>) is prepared by reacting stoichiometric amounts of Al(OH)<sub>3</sub> and MgO with the amine base, triethanolamine (TEAH<sub>3</sub>), in ethylene glycol (EGH<sub>2</sub>). Details of the precursor synthesis are described elsewhere.<sup>16</sup>

The precursor is converted to a ceramic powder by flame spray pyrolysis. This process minimizes process-borne impurities by limiting opportunities for contamination. The process

begins by injecting the precursor into a combustion chamber via an aerosol generator where the individual droplets are rapidly combusted, resulting in the production of crystalline, homogeneous, ultrafine spinel powders. A detailed analysis of the mechanism(s) involved in particle nucleation and growth in the combustion chamber has not been completed; however, the subject has been reviewed for some systems.<sup>17,18</sup> The high-volume throughput of the precursor solution ( $\leq 25$  mL/min at 10 wt% solids loading, solution density  $\approx 0.9$  g/mL), coupled with an apparatus designed for continuous production, leads to production rates of 50–100 g/h. The entire system is low-cost, compact (requires only 3 m<sup>2</sup> of bench-top area), and can be scaled up to achieve higher production rates.

## II. Experimental Procedure

### (1) Equipment

The flame spray pyrolysis system (Figs. 1(a) and (b)) consists of (1) an aerosol generator with fluid feed and reservoir (details follow), (2) a cylindrical quartz combustion chamber, 7.5 cm diameter  $\times$  15 cm, (3) a 5 cm diameter quartz tube ending in a tee, (4) four concentric wire-in-cylinder electrostatic precipitators (ESPs), 5 cm diameter  $\times$  1 m, connected in parallel series, and (5) exhaust piping and flow control valves downstream of the collection zone. The precursor is introduced to the ignition chamber via twin, high-shear fluid (Bernoulli) aerosol generators with oxygen as the atomizing gas. The aerosol generator consists of a 0.4 mm (i.d.) precursor tube oriented perpendicularly to a high-velocity O<sub>2</sub> flow from a 0.8 mm (i.d.) tube (Fig. 1(b)). The twin aerosol generators provide high throughput and stabilize the flame. Two alumina surface-mix natural gas/oxygen pilot torches are used to ignite each aerosol. Torch tip temperatures exceed 2000°C. Downstream temperatures are monitored by Pt–Pt 13% Rh thermocouples (TA Instruments, New Castle, DE) inserted directly into the product stream (Fig. 1(a)); the high flame temperatures do not permit the thermocouple to be placed closer to the combustion zone.

Collection of the ultrafine powders is accomplished using a parallel-series arrangement of wire-in-cylinder electrostatic precipitators. A 5–10 kV dc bias is applied across the 2.5 cm gap between the wire and the wall, inducing electrophoretic deposition of the particles on both the wall and the wire (independent of bias direction). The extremely fine particles and the low bulk density of the agglomerates cause localized filling of the ESPs, restricting gas flow. The use of a parallel-series configuration permits continuous operation, as flow to half of the collection system can be closed temporarily and the filled ESPs replaced without interrupting the process. At full production rates,  $\approx 100$  g/h, each ESP series is replaced for every liter of precursor throughput, alternating every 500 mL. The ESP collection efficiency is 65–75% of total powder production. A countercurrent, packed-bed-column, water scrubber is used to remove the remaining powder from the gas stream, before venting to a hood.

### (2) Precursor Preparation

A double alkoxide precursor to stoichiometric spinel can be prepared by heating an EGH<sub>2</sub> suspension of Al and Mg oxides

G. L. Messing—contributing editor

Manuscript No. 192216. Received November 2, 1995; approved December 28, 1995.

Supported by the Army Materials Laboratory through Contract No. DAAL01-93-M-S522 and by NASA through cooperative research agreement NLRC NCC3-381.

\*Member, American Ceramic Society.

†Address correspondence to this author.

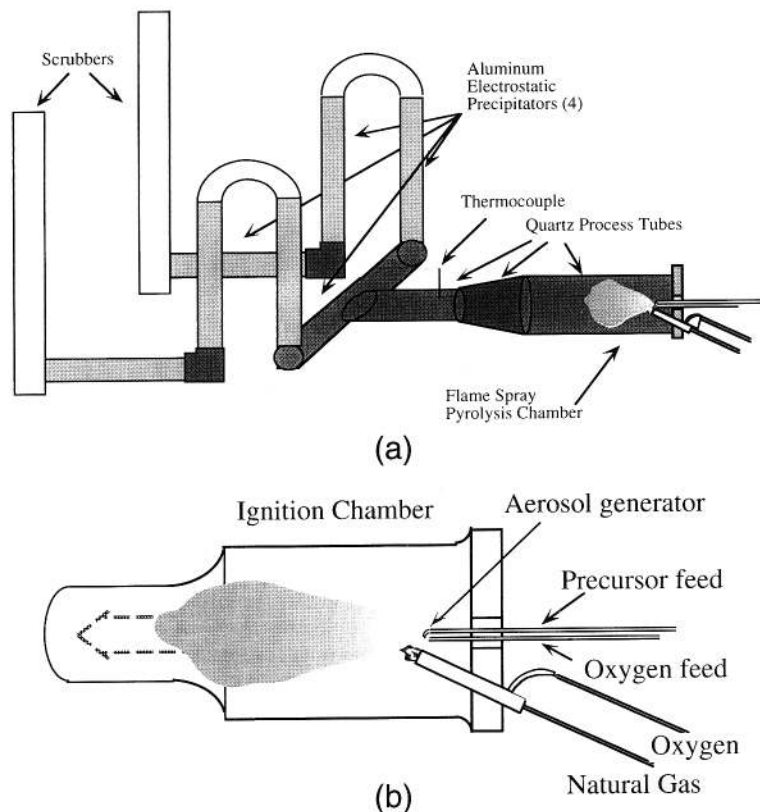


Fig. 1. Schematic of flame spray pyrolysis apparatus.

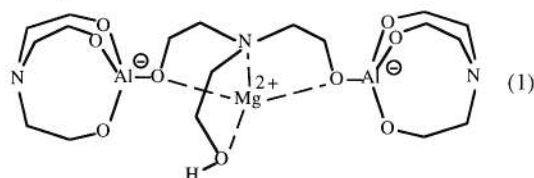
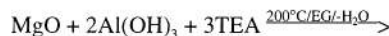
or hydroxides with TEA at 200°C. Reaction proceeds by digesting the starting materials with concurrent distillative removal of byproduct water to form a clear solution. The proposed precursor is a mixture of labile double alkoxide species, such as shown in reaction (1) and identified by high-resolution mass spectroscopy.<sup>16</sup> Two spinel precursors were prepared for this communication. One precursor (SP1) was prepared on a kilogram scale from commercially available  $\text{Al}(\text{OH})_3 \cdot x\text{H}_2\text{O}$  (contains 0.2 wt% Na, Aldrich Chemical Co., Milwaukee, WI) and MgO (Aldrich).<sup>16</sup> A higher-purity precursor (SP2) was prepared from  $\text{Al}(\text{OH})_3 \cdot x\text{H}_2\text{O}$  precipitated from  $\text{AlCl}_3$  (Johnson Matthey, Ward Hill, MA) and  $\text{Mg}(\text{OH})_2$  precipitated from magnesium ethoxide prepared from magnesium metal (Aldrich). Vacuum distillative removal of most of the  $\text{EGH}_2$  solvent provides a viscous polymer-like precursor that can be used directly for flame spray pyrolysis. This precursor gives a TGA ceramic yield of  $\approx 20$  wt% (1000°C/air), which is less than the isolated double alkoxide (27.4 wt% theory)<sup>16</sup> because some residual  $\text{EGH}_2$  is retained. The residual  $\text{EGH}_2$  does not influence the flame pyrolysis results. The as-produced precursor (with  $\text{EGH}_2$ ) is diluted with dry ethanol (EtOH) so that the solution ceramic yield is 4–12 wt%. Precursor viscosity is controlled by the volume of EtOH used, and is critical to proper aerosol generation (see above). EtOH also serves as an additional fuel source for combustion.

### (3) Flame Spray Pyrolysis

The flame spray pyrolysis apparatus converts metal alkoxide precursors into metal oxide powders, and byproduct  $\text{CO}_2$  and  $\text{H}_2\text{O}$ . To avoid  $\text{H}_2\text{O}$  condensation in the collection system, the system is preheated using pure EtOH. When the system has reached steady state (600°C at the combustion chamber thermocouple, TC), the aerosol generator feed is switched to the spinel precursor solution. The precursor flow rate is controlled by application of  $\text{N}_2$  head pressure. EtOH is the primary fuel source; thus, the feed rate determines the combustion chamber temperature. The total production rate is therefore limited by the rate of heat dissipation from the system. Normal operating throughput, using the present configuration, is 20 mL/min (10–12 wt% solution ceramic yield,  $\approx 2$ –5 wt%  $\text{EGH}_2$  in EtOH), or  $\approx 85$  g/h of ceramic powder. Total continuous production for SP1 was  $>1000$  g; as such, some process variability was unavoidable. Total production for SP2 was 50 g.

### III. Results and Discussion

Flame spray pyrolysis effectively produces ultrafine, dense, spherical, homogeneous ceramic powders by rapid combustion of the precursor organic ligands. Primary particles produced from both SP1 and SP2 are  $<100$  nm diameter, roughly spherical polyhedra as shown in Figs. 2(a) and (b), respectively. There



was little or no necking for both SP1 and SP2. The small area diffraction (SAD) patterns of the particles indicate fully crystalline powders. The wide size distributions and spherical shapes, as seen in the Fig. 2 TEMS, are characteristic of gas-phase syntheses.<sup>18</sup>

The specific surface area of the SP1 flame pyrolyzed spinel is 60 m<sup>2</sup>/g by BET. The equivalent spherical diameter predicted from the surface area is 28 nm, while the specific surface area of SP2 derived powder is 40 m<sup>2</sup>/g with a predicted spherical diameter of 42 nm. The XRD powder patterns shown in Fig. 3 indicate that both powders are crystalline spinel. The average crystallite sizes determined using the Debye-Scherrer equation for SP1 and SP2 are 24 and 36 nm, respectively.

The powders from the respective precursors are viewed on a broader scale in the Fig. 4 micrographs. A number of larger (>100 nm) particles (seen as the bright images) exhibit both

hollow and dense spherical morphologies, and appear polycrystalline. The underlying dark material consists of primary particles (Fig. 2). Powder collected during continuous operation (SP1) exhibits a much smaller volume fraction of large particles than the (SP2) run. Recent process improvements have virtually eliminated the larger particles.

The temperatures measured downstream (1–1.5 m) from the combustion zone range from 500° to 700°C and allow a conservative estimate of actual combustion temperatures of 1800–2000°C. These temperatures are not likely to cleave the metal-oxygen bonds in the precursor during pyrolysis; thus, we suggest that M–O bonds (and molecular oxide species) remain intact during pyrolysis. A nucleation and growth mechanism similar to other gas-phase reactions involving these metal oxide species is proposed to operate in the combustion zone.<sup>18</sup> However, no proof, other than the particle morphologies, currently

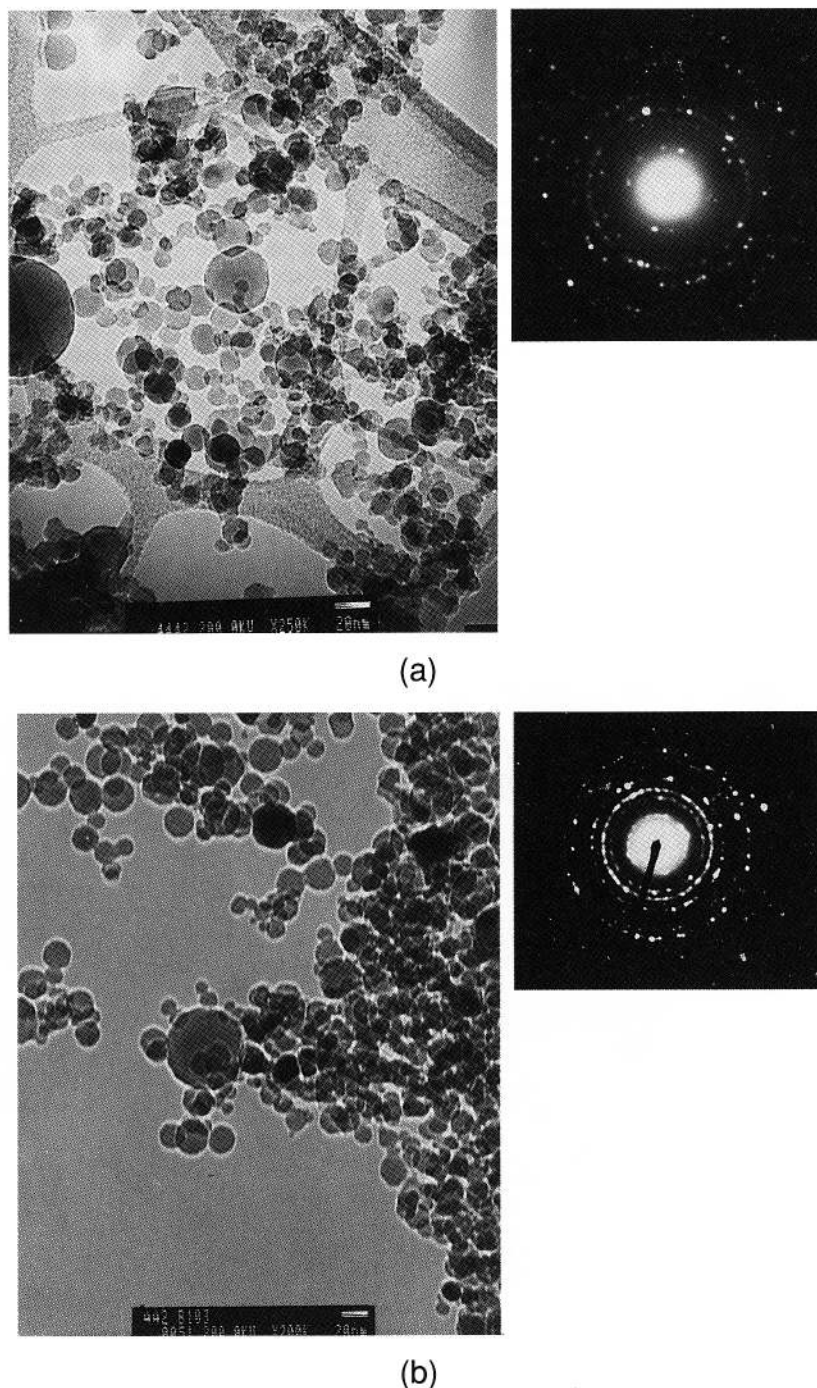


Fig. 2. TEM of (a) SP1 and (b) SP2; insets show small area diffraction patterns.



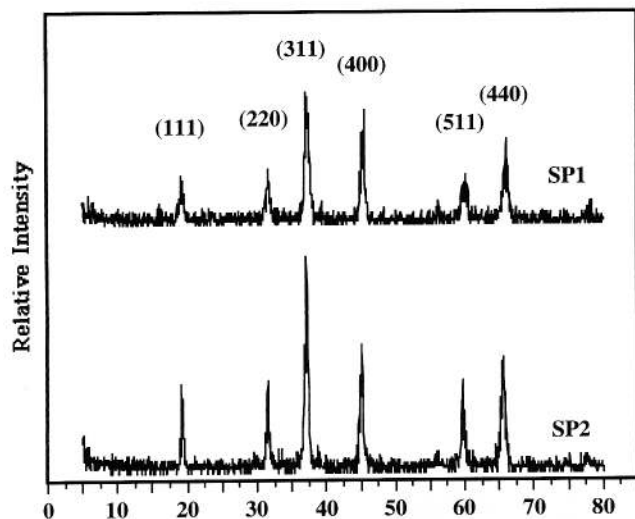


Fig. 3. Powder X-ray diffraction of flame-pyrolyzed spinel.

exists to support our conjectures concerning species formation and particle formation. The average particle diameters derived from SSAs are consistent with the crystallite sizes observed in the TEM and derived from the Debye-Scherrer formula, as shown in Table I.

The chemical homogeneity observed in the powders is likely due to the exact spinel stoichiometry (1Mg:2Al), the atomic homogeneity of the double alkoxide precursor, and the low individual vapor pressures of alumina and magnesia at the processing temperatures involved in the flame pyrolysis process. Lower-temperature processes are known to result in segregated spinel.<sup>15</sup> Combustion of the precursor is rapid; hence, residence time in the flame is short (estimated at <1 s) and the temperature gradient between the flame and the thermocouple is steep (>1000°C/s). The formation of an oxide vapor at temperatures near the melting points of the parent oxides creates a large thermodynamic driving force for rapid nucleation and growth of the solid phase. Al and Mg oxide vapor would be

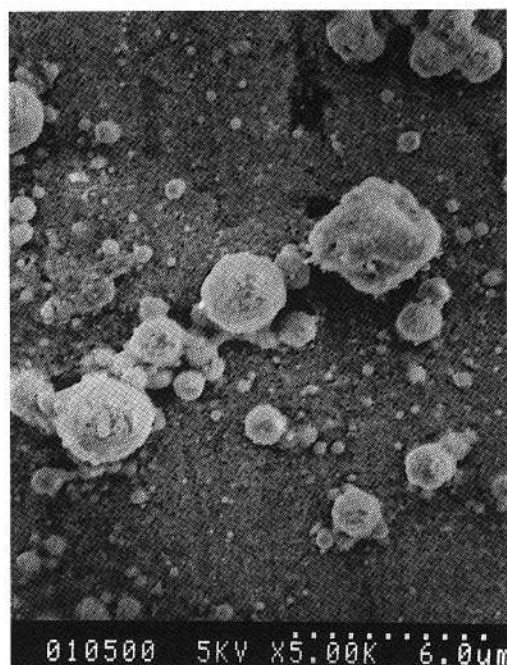
expected to condense homogeneously with the stoichiometry of the local vapor, which is assumed to be a function of the homogeneity of the precursor.

The mechanisms of particle formation appear to be different from those seen in spray pyrolysis.<sup>9</sup> Dense and hollow particles larger than 100 nm, observed by SEM, result from inadequate process control in aerosol generation. Dense particles larger than 100 nm presumably form by coalescence of primary particles in the turbulent combustion chamber. The wide dispersion of droplet sizes produced by the Bernoulli aerosol generator does not appear to directly affect the final particle size or distribution as in spray drying or spray pyrolysis techniques.<sup>9</sup> However, the limiting case of the droplet size is seen when heat transfer is insufficient to volatilize the solvent within the combustion zone. Hollow particles are proposed to result from precursor droplets not immediately vaporized. Evaporation followed by relatively slow combustion of the ethanol and precursor ligands would result in large, hollow particles similar to those sometimes produced by spray pyrolysis. Large droplets or those on the fringe of the mist pattern most likely undergo this process.

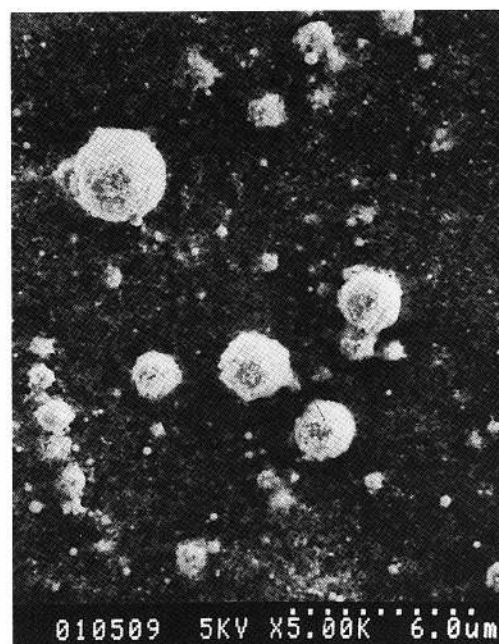
No apparent difference is seen in the properties of the SP1 and SP2 powders, although the SP1 powders<sup>14</sup> retain the sodium impurities (0.2 wt%) originally present in the Al(OH)<sub>3</sub> starting material. These impurities are likely to affect the sintering properties of the resulting powders. However, this observation also suggests that it may be possible to make mixed-metal, ultrafine powders simply by the introduction of the appropriate amount of desired additional metal during the oxide one-pot synthesis of the precursor. Efforts to make β'-alumina via a similar approach are currently under way. Finally, pyrolysis of the bulk precursor and characterization of the resulting bulk ceramic powders by TGA, porosimetry (SSA), XRD, SEM, and TEM will be described in detail elsewhere.<sup>16</sup>

#### IV. Summary

Flame pyrolysis of a magnesium aluminum double alkoxide results in phase pure, nanosized spinel powders. Production rates are 50–100 g/h from a simple bench-top apparatus. Average particle diameters are calculated to be 25–45 nm by equivalent spherical diameter derivation from specific surface area



(a)



(b)

Fig. 4. SEM of (a) SP1 and (b) SP2.

Table I. Summary of the Reaction Conditions and Results of Flame Pyrolysis

Precursor	Ceramic yield (%)	Flow rate (mL/min)	TC1 (K)	Debye-Scherer particle size (nm)	SSA (m <sup>2</sup> /g)	Equiv. spherical diameter SSA (nm)
SP1	8–10	18–20	1200–1400	24	60	28
SP2	4	17	880–1000	36	40	42

data and 24–36 nm by the Debye-Scherer methods. These sizes are consistent with the TEM micrographs. Particles are proposed to form by nucleation and growth of metal oxide species in the vapor phase.

## References

<sup>1</sup>M. R. Gallas, B. Hockey, A. Pechenik, and G. J. Piermarini, "Fabrication of Transparent  $\gamma$ -Al<sub>2</sub>O<sub>3</sub> from Nanosize Particles," *J. Am. Ceram. Soc.*, **77**, 2107–12 (1994).

<sup>2</sup>H. Hahn and R. S. Averback, "Low-Temperature Creep of Nanocrystalline Titanium(IV) Oxide," *J. Am. Ceram. Soc.*, **74**, 1–4 (1991).

<sup>3</sup>H. Gleiter, "Materials with Ultrafine Microstructures: Retrospectives and Perspectives," *Nanostructured Mater.*, **1**, 1–19 (1992).

<sup>4</sup>G. D. Ulrich, "Flame Synthesis of Fine Particles," *Chem. Eng. News*, [August 6] 22–29 (1984).

<sup>5</sup>(a) A. A. Adjaottor and G. L. Griffin, "Aerosol Synthesis of Aluminum Nitride Powder Using Metalorganic Reactants," *J. Am. Ceram. Soc.*, **75**, 3209–14 (1992), and references contained therein. (b) K.-H. Kim, C.-H. Ho, H. Doerr, C. Deshpandey, and R. F. Bunshah, "Ultrafine Aluminum Nitride Powder Produced by Plasma-Assisted Chemical Vapor Deposition of Trimethylaluminum," *J. Mater. Sci.*, **27**, 2580–88 (1992).

<sup>6</sup>G. Skandan, H. Hahn, and J. C. Parker, "Nanostructured Y<sub>2</sub>O<sub>3</sub>: Synthesis and Relation to Microstructure and Properties," *Scr. Met. Mater.*, **25**, 2389–93 (1991).

<sup>7</sup>R. Birringer, H. Gleiter, H. P. Klein, and P. Marquardt, "Nanocrystalline Materials—An Approach to a Novel Solid Structure with Gas-like Disorder?," *Phys. Lett. A*, **102**, 365–69 (1984).

<sup>8</sup>H. Hahn and R. S. Averback, "High Temperature Mechanical Properties of Nanostructured Ceramics," *Nanostructured Mater.*, **1**, 95–100 (1992).

<sup>9</sup>(a) G. L. Messing, S.-C. Zhang, and G. V. Jayanthi, "Ceramic Powder Synthesis by Spray Pyrolysis," *J. Am. Ceram. Soc.*, **76**, 2707–26 (1990).

(b) F. Kirkbir, D. Katz, R. Lysse, and J. D. Mackenzie, "Formation of Dense and Non-agglomerated Lead Oxide Particles by Spray Pyrolysis," *J. Mater. Sci.*, **27**, 1748–56 (1992). (c) K. A. Moore, J. C. Cesarano III, D. M. Smith, and T. T. Kostas, "Synthesis of Submicrometer Mullite Powder via High-Temperature Aerosol Decomposition," *J. Am. Ceram. Soc.*, **75** [1] 213–15 (1992).

<sup>10</sup>A. J. Rulison and R. C. Flagan, "Synthesis of Yttria Powders by Electrospray Pyrolysis," *J. Am. Ceram. Soc.*, **77**, 3244–50 (1994).

<sup>11</sup>J. J. Helble, G. A. Moniz, and J. R. Morency, "Process for Producing Nanoscale Ceramic Powders," U.S. Pat. No. 5 358 695, 1994.

<sup>12</sup>M. J. Mayo, D. C. Hague, and D.-J. Chen, "Processing Nanocrystalline Ceramics for Application in Superplasticity," *Mater. Sci. Eng.*, **A166**, 145–59 (1993).

<sup>13</sup>(a) M. Barj, J. F. Bocquet, K. Chhor, and C. Pommier, "Submicronic MgAl<sub>2</sub>O<sub>4</sub> Powder Synthesis in Supercritical Ethanol," *J. Mater. Sci.*, **27**, 2187–92 (1992). (b) H. Cheng, J. Ma, Z. Zhao, and L. Qi, "Hydrothermal Preparation of Uniform Nanosize Rutile and Anatase Particles," *Chem. Mater.*, **7**, 663–71 (1995).

<sup>14</sup>R. M. Laine, D. R. Treadwell, B. Mueller, and T. Hinklin; unpublished results.

<sup>15</sup>N. Yang and L. Chang, "Structural Inhomogeneity and Crystallization Behavior of Aerosol-Reacted MgAl<sub>2</sub>O<sub>4</sub> Powders," *Mater. Lett.*, **15**, 84–88 (1992).

<sup>16</sup>K. Waldner, R. M. Laine, C. Bickmore, R. Narayanan, S. Dumrongvaraporn, and S. Tayaniphan, "Synthesis, Processing and Pyrolytic Transformation of a Spinel Polymer Precursor Made from MgO and Al(OH)<sub>3</sub>," submitted for publication.

<sup>17</sup>(a) K. A. Kusters and S. E. Pratsinis, "Strategies for Control of Ceramic Powder Synthesis by Gas-to-Particle Conversion," *Powder Technol.*, **82**, 79–91 (1995). (b) J. J. Wu, H. V. Nguyen, R. C. Flagan, K. Okuyama, and Y. Kousaka, "Evaluation and Control of Particle Properties in Aerosol Reactors," *AIChE J.*, **34**, 1249–58 (1988).

<sup>18</sup>A. Gurav, T. Kostas, T. Pluym, and Y. Xiong, "Aerosol Processing of Materials," *Aerosol Sci. Technol.*, **19**, 411–52 (1993). □